symmetry

MDPI

*Article*

# An Axi-Symmetric Problem of Suspensions Filtering with the Formation of a Cake Layer

**Bakhtiyor Kh. Khuzhayorov [1,2], Gafurjan Ibragimov [3], Usmonali Saydullaev [1] and Bruno Antonio Pansera [4,*]**

[1] Department of Mathematical Modeling, Samarkand State University, University Blv. 15, Samarkand 140104, Uzbekistan; b.khuzhayorov@mail.ru (B.K.K.); saydullayev@samdu.uz (U.S.)
[2] V.I. Romanovski Institute of Mathematics, Academy of Sciences, Tashkent 100174, Uzbekistan
[3] Department of General and Exact Subjects, Tashkent State University of Economics, Tashkent 100066, Uzbekistan; gofurjon.ibragimov@tsue.uz
[4] Department of Law and Economics, University "Mediterranea" of Reggio Calabria, 89124 Reggio Calabria, Italy
* Correspondence: bruno.pansera@unirc.it

**Abstract:** In this paper, we consider a vertically positioned cylindrical filtering element. Filtering occurs in the radial direction, therefore, the direction of the velocities of the liquid and suspended particles coincide with this radial direction. The flow can be considered to be one-dimensional and radially axisymmetric. To describe such a filtering process, the axisymmetric Stefan problem will be formulated. The radial mass balance formalism and Darcy's law are utilized to obtain a basic equation for cake filtration. The boundary condition at the moving surface is derived and the cake filtration is formulated in a Stefan problem. Equations are derived that describe the dynamics of cake growth in the cake filtration, and they are numerically solved. The influence of different model parameters on the compression and fluid pressure across the cake and the growth of its thickness are studied.

**Keywords:** cake characteristics; cake filtration; concentration; permeability; porosity; compression pressure



**Citation:** Khuzhayorov, B.K.; Ibragimov, G.; Saydullaev, U.; Pansera, B.A. An Axi-Symmetric Problem of Suspensions Filtering with the Formation of a Cake Layer. *Symmetry* **2023**, *15*, 1209. https://doi.org/10.3390/sym15061209

Academic Editors: Iver H. Brevik, Sergei Alexandrov and Sergei D. Odintsov

Received: 10 April 2023
Revised: 20 May 2023
Accepted: 31 May 2023
Published: 5 June 2023



## 1. Introduction

Filtration is the process of separating heterogeneous systems using a porous septum, which delays some phases of these systems and passes others. These processes include the separation of the suspension into a clean liquid and sediment. The separation of the suspension in which solid particles are suspended is carried out using a filter. Suspension separation processes are found in chemical, petrochemical, oil refining, coal, food, and other industries [1–11].

The most important characteristic of suspensions affecting the type and intensity of filtration is the concentration of the solid phase, which is expressed in fractions of volume or mass. Depending on the concentration of the solid phase in the suspension, the types of filtration are distinguished [1–3]: with the formation of a precipitate, it is intermediate, and with the clogging of the pores of the precipitate, it is gradual, as well as with a complete clogging of the pores of the filter partition. Solids contained in the suspension are retained on the surface of the septum and form a layer of sediment.

Filtering with the formation of a cake is based on the fundamental equations of the mechanics of multicomponent media and the theory of filtration consolidation, taking into account the influence of hydrodynamic and rheological factors on the laws of the filtering process [5,6].

In the theory of filtering, the main averaged characteristics are the filtering velocity and the pressure. The process of suspension flow in a porous medium is described by Darcy's law. In [12–15], the averaged equations for the mechanics of two-phase flows were

given, and filtering equations were obtained. In [1,4], dynamic equations were obtained via a statistical averaging of the equations for the mechanics of two-phase flows, taking into account the inertial effects during filtering. The differential filtering equations in [7,12–17] were obtained on the basis of the equations for the mechanics of two-phase flows and soil mechanics, taking into account the change in the filtration parameters over the thickness of the sediment and over time.

Since in the process of filtering, the sediment–suspension interface is mobile, the models are usually reduced to Stefan problems [1,4,7], the numerical solution of which, as is known, has a number of specific features [18–24].

When filtering the clarification of a suspension, one of the main technical elements are the filters, the design and technical characteristics of which can be different [1,4]. In this case, particles of the suspension either linger on the surface of the filter, forming a precipitate called a cake, or penetrate the filter, lingering in the pores. In accordance with this, filtering is distinguished by the formation of a cake and filtering with clogged pores [1,2,4]. The filter element often has a cylindrical shape, through which a suspension is supplied through the inner- or outer-side surface.

In this paper, the axisymmetric problem of suspension filtration is considered, taking into account the consolidation of the cake. We use here a geometric schematization of the filter, as seen in [5]. To compose a mathematical model, we use the methodology developed in [1–3]. Thus, for the first time, filtration equations are derived in a radially symmetric case, taking into account the consolidation of the cake. A suspension filtering problem through a radial filter with a given pressure at the interface between the suspension and the cake is set. The problem is solved numerically using the finite difference method. Since the Stefan problem is obtained for the growth of the cake thickness, a special method of "catching the front" is applied to determine it. The pressure fields in the liquid and solid phases of the cake, the relative permeability of the cake, the concentration of the solid particles in the cake, and the thickness of the cake, as well as other filtering characteristics, are determined. The influence of the parameters on the dependencies of the cake solid concentration and the permeability of the pressure in the solid phases on the filtration characteristics are studied.

## 2. Physical Model

Here, we consider the process of filtering suspensions through a cylindrical filter (Figure 1). The suspension is fed through the outer surface of the filter, with a radius $R$, upon which the cake is formed. The relative contents of the liquid and solid phases are denoted by $\varepsilon$ and $\varepsilon_s$, $\varepsilon + \varepsilon_s = 1$. The filtration velocities for the liquid and solid phases are denoted by $q_\ell$ and $q_s$, respectively.

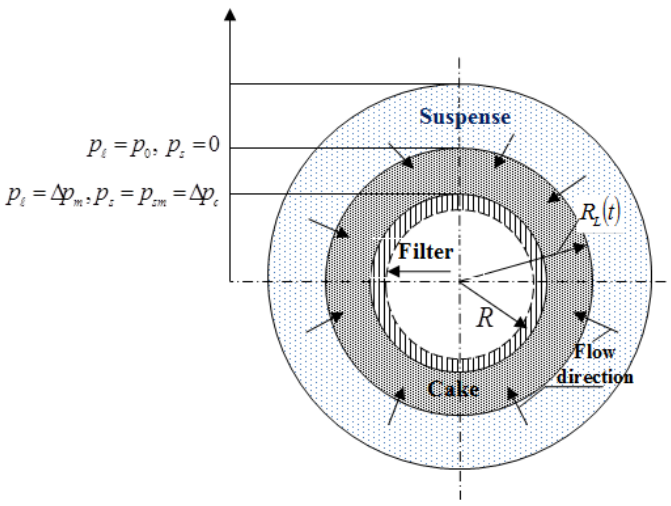


**Figure 1.** A schematic of filtering suspensions through a cylindrical filter.

## 3. Mathematical Model

Here, we give the derivation of the filtering equation. We suppose that the filtering occurs in the radial direction, which means that the direction of the velocities of the liquid and suspended particles coincide with this radial direction. Therefore, we ignore the angular flow of the suspension in our adopted scheme (geometry) for the filtering and consider it as one-dimensional. Multi-dimensional equations arise in non-symmetrical flows of suspension with the formation of the cake [5]. Thus, the continuity equations of the fluid and particle phases in a cylindrical coordinate system can be written as [1–5]:

$$\frac{\partial \varepsilon}{\partial t} + \frac{1}{2\pi r}\frac{\partial q_\ell}{\partial r} = 0, \tag{1}$$

$$\frac{\partial \varepsilon_s}{\partial t} + \frac{1}{2\pi r}\frac{\partial q_s}{\partial r} = 0, \tag{2}$$

where $t$ is time and $r$ is the radial coordinate.

Since $\varepsilon + \varepsilon_s = 1$, by adding Equations (1) and (2), we obtain:

$$\frac{\partial q_\ell}{\partial r} + \frac{\partial q_s}{\partial r} = 0,$$

where:

$$q_\ell + q_s = q_{out}, \tag{3}$$

$q_{out}$, is the instantaneous filtration velocity, independent of the coordinate $r$.

The Darcy law for axisymmetric filtering is as follows [1,5]:

$$q_\ell - \frac{\varepsilon}{\varepsilon_s} q_s = -2\pi r \frac{k}{\mu}\frac{\partial p_\ell}{\partial r}, \tag{4}$$

where $p_\ell$ is the liquid pressure, $\mu$ is the fluid viscosity, and $k$ is the cake permeability.

Upon differentiating Equation (4) by $r$, we obtain:

$$\frac{\partial q_\ell}{\partial r} = -\frac{\partial}{\partial r}\left(2\pi r \frac{k}{\mu}\frac{\partial p_\ell}{\partial r} - \frac{\varepsilon}{\varepsilon_s} q_s\right). \tag{5}$$

Assuming that the particle velocity is zero at the boundary of the filter and the cake ($q_s|_{r=R} = 0$), at each point in the cake, we have:

$$q_\ell + q_s = q_{out} = -\left[2\pi r \frac{k}{\mu}\frac{\partial p_\ell}{\partial r}\right]_{r=R} = \frac{-p_{\ell m}}{\mu R_m}, \tag{6}$$

where $R$ is the outer radius of the filter element, $p_{\ell m}$ is the filtrate pressure at $r = R$, and $R_m$ is the medium resistance.

From Equations (4) and (6), we can see:

$$q_s = \varepsilon_s \left\{2\pi r \frac{k}{\mu}\frac{\partial p_\ell}{\partial r} - \left[2\pi r \frac{k}{\mu}\frac{\partial p_\ell}{\partial r}\right]_{r=R}\right\}. \tag{7}$$

By substituting (7) into (5), we obtain:

$$\frac{\partial q_\ell}{\partial r} = -\frac{\partial}{\partial r}\left(\varepsilon_s 2\pi r \frac{k}{\mu}\frac{\partial p_\ell}{\partial r} + (1-\varepsilon_s)\left[2\pi r \frac{k}{\mu}\frac{\partial p_\ell}{\partial r}\right]_{r=R}\right)$$

or

$$\frac{\partial q_\ell}{\partial r} = -\frac{\partial}{\partial r}\left(\varepsilon_s 2\pi r \frac{k}{\mu}\frac{\partial p_\ell}{\partial r}\right) - \left[2\pi r \frac{k}{\mu}\frac{\partial p_\ell}{\partial r}\right]_{r=R}\frac{\partial \varepsilon_s}{\partial r}.$$

Using (1) and (2), we obtain:

$$\frac{\partial \varepsilon_s}{\partial t} = -\frac{1}{r}\frac{\partial}{\partial r}\left(\varepsilon_s \cdot r\frac{k}{\mu}\frac{\partial p_\ell}{\partial r}\right) - \frac{q_{out}}{2\pi}\cdot\frac{1}{r}\frac{\partial \varepsilon_s}{\partial r}, \tag{8}$$

where $q_{out} = \left[-2\pi r\frac{k}{\mu}\frac{\partial p_\ell}{\partial r}\right]_{r=R}$ is the instantaneous filtration velocity.

Equation (8) is the basic filtration equation with the formation of a cake in cylindrical coordinates. It can be solved with corresponding initial and boundary conditions, specified, in particular, on the moving boundary $r = R_L(t)$, which must be determined from the additional equation.

The properties of the cake are characterized by several parameters [1,3,7,8,12]: the volume fraction of the particle, the solidosity (particle volume fraction) $\varepsilon_s$, or the cake permeability $k$. These parameters are assumed to only be functions of the cake compressive stress $p_s$

$$\varepsilon_s = \varepsilon_s(p_s),\ k = k(p_s).$$

In particular, the following power law expressions may be used [3,7,8,12]:

$$\varepsilon_s = \varepsilon_s^0\left(1 + \frac{p_s}{p_A}\right)^{\beta}, \tag{9}$$

$$k = k^0\left(1 + \frac{p_s}{p_A}\right)^{-\delta}, \tag{10}$$

where $\varepsilon_s^0$ and $k^0$ denote, respectively, the values of $\varepsilon_s$, $k$, and $\alpha$ at $p_s = 0$, respectively; $p_A$ is the specific stress and the indicators $\beta$, $\delta$, and $n = \delta - \beta$ are constant values.

Neglecting friction forces, the following relationships between $p_\ell$ and $p_s$ [3] can be used:

$$\text{Type 1}: \ dp_\ell + dp_s = 0, \tag{11a}$$

$$\text{Type 2}: \ (1-\varepsilon_s)dp_\ell + dp_s = 0, \tag{11b}$$

$$\text{Type 3}: \ (1-\varepsilon_s)dp_\ell + \varepsilon_s dp_s = 0, \tag{11c}$$

$$\text{Type 4}: \ d[(1-\varepsilon_s)p_\ell] + d[\varepsilon_s p_s] = 0. \tag{11d}$$

At the borders of the cake, the following conditions are applied: $p_\ell = p_0$ when $r = R_L(t)$ and $p_\ell = \Delta p_m$ when $r = 0$, where $\Delta p_m$ is the differential pressure through the filter element.

From (11a)–(11d), we have:

$$\frac{\partial p_\ell}{\partial p_s} = f', \tag{12}$$

where:

$$f' = -1, \qquad \text{for Type 1,} \tag{13a}$$

$$f' = -\frac{1}{1-\varepsilon_s}, \qquad \text{for Type 2,} \tag{13b}$$

$$f' = -\frac{\varepsilon_s}{1-\varepsilon_s}, \qquad \text{for Type 3,} \tag{13c}$$

$$f' = \frac{\left(1-\varepsilon_s^0\right)p_0 - p_s}{\left(1-\varepsilon_s\right)^2}\frac{d\varepsilon_s}{dp_s} - \frac{\varepsilon_s}{1-\varepsilon_s}, \quad \text{for Type 4.} \tag{13d}$$

From (8), (9), (10), and (13a), we obtain:

$$\frac{\partial \varepsilon_s}{\partial t} = -\frac{1}{r}\frac{\partial}{\partial r}\left(\varepsilon_s^0 \cdot r\frac{k^0}{\mu}\left(\frac{\varepsilon_s}{\varepsilon_s^0}\right)^{-\delta/\beta} f'\frac{\partial p_s}{\partial r}\right) - \frac{q_{out}}{2\pi}\cdot\frac{1}{r}\frac{\partial \varepsilon_s}{\partial r}. \tag{14}$$

The equation for the increasing radius $R_L(t)$, which expresses the thickness of the cylindrical cake, that is, the radius of the boundary between the suspension and the cake, is given in the following form:

$$\frac{dR_L}{dt} = \frac{\varepsilon_s^0}{\varepsilon_s^0 - \varepsilon_{s_0}}\left[\frac{k}{\mu}\frac{\partial p_\ell}{\partial r}\right]_{r=R_{L^-}} + \frac{1}{2\pi R_{L^-}} q_{out}, \tag{15}$$

On the surface $r = R_{L^-}$, the stresses of the compressing particles are zero. That is, $\varepsilon_s|_{R_{L^-}}$ can be taken as equal to the solid content at zero stress $\varepsilon_s^0$. On the other hand, $\varepsilon_s|_{R_{L^+}}$ is equal to the concentration of the solids in the suspension $\varepsilon_{s_0}$.

If the process begins in a new filter without first pumping the liquid, we can accept the initial condition:

$$R_L(0) = R. \tag{16}$$

The filtering process begins with a sudden application of pressure or a set flow rate. The initial conditions for $p_\ell$ and $p_s$ can be taken as zero, i.e.,

$$p_\ell(0, r) = 0,\ p_s(0, r) = 0. \tag{17}$$

The boundary conditions for an axisymmetric problem are:

$$p_\ell = p_0,\ p_s = 0,\ \varepsilon_s = \varepsilon_s^0 \text{ when } r = R_L(t), \tag{18a}$$

$$-2\pi r\frac{k}{\mu}\frac{\partial p_\ell}{\partial r} = \frac{-p_\ell}{R_m \mu} \text{ when } r = R. \tag{18b}$$

When the fluid flow rate is set:

$$p_s = 0,\ \varepsilon_s = \varepsilon_s^0 \text{ when } r = R_L(t), \tag{19a}$$

$$-2\pi r\frac{k}{\mu}\frac{\partial p_\ell}{\partial r} = -\frac{-p_\ell}{R_m \mu} = \text{const when } r = R. \tag{19b}$$

When the filtering has a variable pressure, we have:

$$p_\ell = p(t),\ p_s = 0,\ \varepsilon_s = \varepsilon_s^0 \text{ when } r = R_L(t), \tag{20a}$$

$$-2\pi r\frac{k}{\mu}\frac{\partial p_\ell(t)}{\partial r} = -\frac{p_\ell(t)}{R_m \mu} \text{ when } r = R. \tag{20b}$$

In the preset pressure mode, it is possible to calculate the filtrate flow rate at the filter outlet $q_{out} = \left[-2\pi r\frac{k}{\mu}\frac{\partial p_\ell}{\partial r}\right]_{r=R}$, as it is a function of time.

## 4. Numerical Analysis

Using (9)–(10), we can obtain from (8) the equation for $p_s$:

$$\frac{\beta\varepsilon_s^0}{p_A}\left(1+\frac{p_s}{p_A}\right)^{\beta-1}\frac{\partial p_s}{\partial t} = -\frac{\varepsilon_s^0 k^0}{\mu}\frac{1}{r}\frac{\partial}{\partial r}\left(\left(1+\frac{p_s}{p_A}\right)^{\beta-\delta} r\frac{\partial p_\ell}{\partial r}\right) + \frac{\beta\varepsilon_s^0}{p_A}\left(1+\frac{p_s}{p_A}\right)^{\beta-1}\frac{q_{out}}{2\pi}\cdot\frac{1}{r}\frac{\partial p_\ell}{\partial r}, \tag{21}$$

where:

$$q_{out} = -2\pi r \frac{k^0}{\mu}\left(1+\frac{p_s}{p_A}\right)^{-\delta}\frac{\partial p_\ell}{\partial r}\bigg|_{r=R} = 2\pi r \frac{k^0}{\mu}\left(1+\frac{p_s}{p_A}\right)^{-\delta}\frac{\partial p_s}{\partial r}\bigg|_{r=R}.$$

In the case of $f' = -1$ (Type 13a) from (1), we have:

$$\frac{\beta\varepsilon_s^0}{p_A}\left(1+\frac{p_s}{p_A}\right)^{\beta-1}\frac{\partial p_s}{\partial t} = \frac{\varepsilon_s^0 k^0}{\mu}\frac{1}{r}\frac{\partial}{\partial r}\left(\left(1+\frac{p_s}{p_A}\right)^{\beta-\delta} r\frac{\partial p_s}{\partial r}\right) + \frac{\beta\varepsilon_s^0}{p_A}\left(1+\frac{p_s}{p_A}\right)^{\beta-1}\frac{q_{out}}{2\pi}\cdot\frac{1}{r}\frac{\partial p_s}{\partial r}. \quad (22)$$

We consider the filtering mode with a given pressure, which corresponds to the conditions in (18). From (18a), we obtain the boundary conditions for $p_s$:

$$-2\pi\left[r\frac{k}{\mu}\frac{\partial p_s}{\partial r}\right]_{r=R} = \frac{p_0 - p_s}{\mu R_m}\bigg|_{r=R},\ p_s(t, R_L(t)) = 0, \quad (23)$$

We write Equation (22) in the following form:

$$\frac{\partial p_s}{\partial t} = \frac{p_A k^0}{\beta\mu}\left(1+\frac{p_s}{p_A}\right)^{1-\beta}\frac{1}{r}\frac{\partial}{\partial r}\left(\left(1+\frac{p_s}{p_A}\right)^{\beta-\delta} r\frac{\partial p_s}{\partial r}\right) + \frac{q_{out}}{2\pi}\cdot\frac{1}{r}\frac{\partial p_s}{\partial r}. \quad (24)$$

We introduce the following notations:

$$a(p) = \frac{p_A k^0}{\beta\mu}\left(1+\frac{p_s}{p_A}\right)^{1-\beta},\ b(p) = \left(1+\frac{p_s}{p_A}\right)^{\beta-\delta},\ c(p) = \frac{\varepsilon_s^0}{\varepsilon_s^0 - \varepsilon_{s_0}}\frac{k^0}{\mu}\left(1+\frac{p_s}{p_A}\right)^{-\delta},$$

$$c^0(p) = \frac{k^0}{\mu}\left(1+\frac{p_s}{p_A}\right)^{-\delta}\bigg|_{r=R}.$$

Given these notations, Equation (24) can be transformed into the following form:

$$\frac{\partial p_s}{\partial t} = a(p)\frac{1}{r}\frac{\partial}{\partial r}\left(b(p) r\frac{k}{\mu}\frac{\partial p_s}{\partial r}\right) - \frac{q_{out}}{2\pi}\cdot\frac{1}{r}\frac{\partial p_s}{\partial r}. \quad (25)$$

The equation for the moving boundary $R_L(t)$, (15), takes the form:

$$\frac{dR_L}{dt} = c(p)\left[\frac{\partial p_\ell}{\partial r}\right]_{r=R_{L^-}} + \frac{1}{2\pi R_{L^-}}q_{out}, \quad (26)$$

where $q_{out} = \left[-c^0(p)2\pi r\frac{\partial p_\ell}{\partial r}\right]_{r=R}$.

To solve the problems in (25) and (26), we use the finite differences method [19,20,23,24]. We introduce a uniform grid using $t$ with the step $\tau$:

$$\overline{\omega}_\tau = \{t|\ t = t_j = j\tau,\ j = 0, 1, \ldots, N,\ \tau N = T\},$$

and a non-uniform grid with the coordinate $r$,

$$\overline{\omega}_h = \{r|\ r = r_i = r_{i-1} + h_i,\ i = 1, 2, \ldots, N,\ r_N = R_{L^-}\},$$

with the variable step $h_i > 0$. We choose the step $h_i$ from the interval $[r_i,\ r_{i+1}]$ so that the moving boundary moves exactly on one step along the time grid. This approach is known as the method of catching the front in a grid node. We denote the grid function corresponding to $p_s$ by $\Phi_i^{j+1}$. We approximate Equation (25) using an implicit difference scheme that is nonlinear, with respect to the function $\Phi_i^{j+1}$

$$\frac{\Phi_i^{j+1}-\Phi_i^j}{\tau}=\frac{a\left(\Phi_i^j\right)}{r_i}\frac{2}{h_i+h_{i+1}}\left\{b(\Phi_{i+1/2}^{j+1})r_{i+1/2}\frac{\Phi_{i+1}^{j+1}-\Phi_i^{j+1}}{h_{i+1}}-b(\Phi_{i-1/2}^{j+1})r_{i-1/2}\frac{\Phi_i^{j+1}-\Phi_{i-1}^{j+1}}{h_i}\right\}-(q_{out})_0^{j+1}\frac{1}{2\pi r_i}\frac{\Phi_i^{j+1}-\Phi_{i-1}^{j+1}}{h_i},\quad i=1,\ldots,N-1,j=0,1,\ldots,N-1,\ j=0,1,\ldots,N-1, \tag{27}$$

where:

$$r_{i-1/2}=\frac{r_{i-1}+r_i}{2},\ r_{i+1/2}=\frac{r_{i+1}+r_i}{2},\ a\left(\Phi_i^j\right)=\frac{p_A k^0}{\beta\mu}\left(1+\frac{\Phi_i^j}{p_A}\right)^{1-\beta},\ (q_{out})_0^{j+1}=-2\pi r_1 c^0\left(\Phi_0^{j+1}\right)\left(\frac{\Phi_1^{j+1}-\Phi_0^{j+1}}{h_0}\right),$$

$$b\left(\Phi_{i+1/2}^{j+1}\right)=\frac{1}{2}\left[\left(1+\frac{\Phi_{i+1}^{j+1}}{p_A}\right)^{\beta-\delta}+\left(1+\frac{\Phi_i^{j+1}}{p_A}\right)^{\beta-\delta}\right],\ c^0\left(\Phi_0^{j+1}\right)=\frac{k^0}{\mu}\left(1+\frac{\Phi_0^{j+1}}{p_A}\right)^{-\delta}.$$

Using the approximation $\frac{dR_L}{dt}\approx\frac{h_{i+1}}{\tau}$, Equation (26) can be written in the form:

$$\frac{h_{i+1}}{\tau}=-\left[c\left(\Phi_{i-1/2}^j\right)\left(\frac{\Phi_i^{j+1}-\Phi_{i-1}^{j+1}}{h_{i+1}}\right)\right]-\frac{1}{2\pi r_i}(q_{out})_0^{j+1}, \tag{28}$$

where:

$$c\left(\Phi_{i-1/2}^j\right)=\frac{\varepsilon_s^0}{\varepsilon_s^0-\varepsilon_{s_0}}\frac{k^0}{2\mu}\left[\left(1+\frac{\Phi_i^j}{p_A}\right)^{-\delta}+\left(1+\frac{\Phi_{i-1}^j}{p_A}\right)^{-\delta}\right].$$

An approximation of the initial (17) and boundary conditions (23) gives:

$$\begin{gathered}\Phi_i^{j+1}=0,\ i=0,1,\ldots,N,\ j=0,\\ -2\pi r_1 c^0\left(\Phi_0^j\right)\frac{\Phi_1^{j+1}-\Phi_0^{j+1}}{h_1}=\frac{p_0-\Phi_0^{j+1}}{R_m},j=\overline{0,N},\\ \Phi_i^{j+1}=0,\ i=N+1,\ N+2,\ \ldots,\ j=0,1,\ldots.\end{gathered} \tag{29}$$

The obtained set of Equation (27) are nonlinear, and so to solve them, we use the method of simple iteration and rewrite the system of Equation (27) as follows:

$$\begin{aligned}\frac{\overset{(\lambda+1),j+1}{\Phi}_i-\Phi_i^j}{\tau}&=\frac{a\left(\Phi_i^j\right)}{r_i}\frac{2}{h_i+h_{i+1}}\left\{b\left(\overset{(\lambda),j+1}{\Phi}_{i+1/2}\right)r_{i+1/2}\frac{\overset{(\lambda+1),j+1}{\Phi}_{i+1}-\overset{(\lambda+1),j+1}{\Phi}_i}{h_{i+1}}-b\left(\overset{(\lambda),j+1}{\Phi}_{i-1/2}\right)r_{i-1/2}\frac{\overset{(\lambda+1),j+1}{\Phi}_i-\overset{(\lambda+1),j+1}{\Phi}_{i-1}}{h_i}\right\}\\&-\left(\overset{(\lambda)}{q_{out}}\right)_0^{j+1}\frac{1}{2\pi r_i}\frac{\overset{(\lambda+1),j+1}{\Phi}_i-\overset{(\lambda+1),j+1}{\Phi}_{i-1}}{h_i},i=1,\ldots,N-1,\ j=0,1,\ldots,N-1,\end{aligned} \tag{30}$$

where:

$$b\left(\overset{(\lambda),j+1}{\Phi}_{i+1/2}\right)=\frac{1}{2}\left[\left(1+\frac{\overset{(\lambda),j+1}{\Phi}_{i+1}}{p_A}\right)^{\beta-\delta}+\left(1+\frac{\overset{(\lambda),j+1}{\Phi}_i}{p_A}\right)^{\beta-\delta}\right],\ \left(\overset{(\lambda)}{q_{out}}\right)_1^{j+1}=2\pi r_1 c^0\overset{(\lambda),j+1}{\Phi}_0\left(\frac{\overset{(\lambda),j+1}{\Phi}_1-\overset{(\lambda),j+1}{\Phi}_0}{h_0}\right),$$

$\lambda$ is the number of iterations.

It can be seen that the system of Equation (30) is now linear with respect to $\overset{(\lambda+1),j+1}{\Phi}_i$, which allows us to use the Thomas algorithm. As a condition for stopping the iteration procedure on this time layer, the following relationship can be used:

$$\max_i \left| \overset{(\lambda+1),j+1}{\Phi}_i - \overset{(\lambda),j+1}{\Phi}_i \right| \le \Lambda, \tag{31}$$

where $\Lambda$ is the exact calculation. If condition (31) is satisfied, then $\overset{(\lambda+1),j+1}{\Phi}_i = \Phi_i^{j+1}$. As an initial approach, we can take $\overset{(\lambda=0),j+1}{\Phi}_i = \Phi_i^j$.

Equation (30) leads to the system of linear equations:

$$\overset{(\lambda)}{A_i} \cdot \overset{(\lambda+1),j+1}{\Phi}_{i-1} - \overset{(\lambda)}{B_i} \cdot \overset{(\lambda+1),j+1}{\Phi}_i + \overset{(\lambda)}{C_i} \cdot \overset{(\lambda+1),j+1}{\Phi}_{i+1} = -\overset{(\lambda)}{F_i}, \; i = \overline{1, N-1}, \tag{32}$$

where $\overset{(\lambda)}{A_i} = \frac{a\left(\Phi_i^j\right)}{r_i} \frac{2}{h_i+h_{i+1}} \frac{b\left(\overset{(\lambda),j+1}{\Phi}_{i-1/2}\right)}{h_i} r_{i-1/2} + \left(\overset{(\lambda)}{q_{out}}\right)_i^{j+1} \frac{1}{2\pi r_i h_i}$, $\overset{(\lambda)}{C_i} = \frac{a\left(\Phi_i^j\right)}{r_i} \frac{2}{h_i+h_{i+1}} \frac{b\left(\overset{(\lambda),j+1}{\Phi}_{i+1/2}\right)}{h_{i+1}} r_{i+1/2}$,

$\overset{(\lambda)}{B_i} = \frac{1}{\tau} + \frac{a\left(\Phi_i^j\right)}{r_i} \frac{2}{h_i+h_{i+1}} \left[ \frac{b\left(\overset{(\lambda),j+1}{\Phi}_{i+1/2}\right)}{h_{i+1}} r_{i+1/2} + \frac{b\left(\overset{(\lambda),j+1}{\Phi}_{i-1/2}\right)}{h_i} r_{i-1/2} \right] + \left(\overset{(\lambda)}{q_{out}}\right)_0^{j+1} \frac{1}{2\pi r_i h_i}$, $\overset{(\lambda)}{F_i} = \frac{1}{\tau}\Phi_i^j$.

Equation (28) is used to determine the step $h_{i+1}$, which can be written in the form:

$$(h_{i+1})^2 - \frac{\tau}{2\pi r_i} (q_{out})_0^{j+1} h_{i+1} - \tau c \left(\Phi_{i-1/2}^j\right) \left(\Phi_i^{j+1} - \Phi_{i-1}^{j+1}\right) = 0. \tag{33}$$

By solving this nonlinear equation for $h_{i+1}$ for each temporal, the system of linear algebraic Equation (32) is solved by the Thomas algorithm:

$$\overset{(\lambda+1),j+1}{\Phi}_i = \xi_{i+1} \overset{(\lambda+1),j+1}{\Phi}_{i+1} + \eta_{i+1}, \tag{34}$$

where $\xi_{i+1} = \frac{\overset{(\lambda)}{C_i}}{\overset{(\lambda)}{B_i} - \overset{(\lambda)}{A_i}\xi_i}$, $\eta_{i+1} = \frac{\overset{(\lambda)}{F_i} + \overset{(\lambda)}{A_i}\eta_i}{\overset{(\lambda)}{B_i} - \overset{(\lambda)}{A_i}\xi_i}$.

## 5. Numerical Results

Using (32)–(33), the numerical results can be obtained corresponding to the following parameter values: $p_A = 10^4$ Pa, $R_m = 10^{12}$ 1/m$^2$, $\mu = 10^{-3}$ Pa $\cdot$ s, $k^0 = 10^{-13}$ m$^2$, $\varepsilon_s^0 = 0.20$, and $\varepsilon_{s_0} = 0.0076$. Some results are shown in Figures 2–10. As can be seen from the presented results, as the filtering process continues, the thickness of the cake increases and the distribution of the compression pressure and fluid pressure is established over the entire thickness. In accordance with the assumptions made, the compression pressure decreases from the filter surface to the boundary of the cake and suspension. The pressure in the liquid on the surface of the filter has a value of $p_\ell = \Delta p_m$ and this value increases to $p_0$ at the common border of the cake and suspension. The graphs in Figures 2 and 3 have an exact ending determined by the moving front of $R_L(t)$.

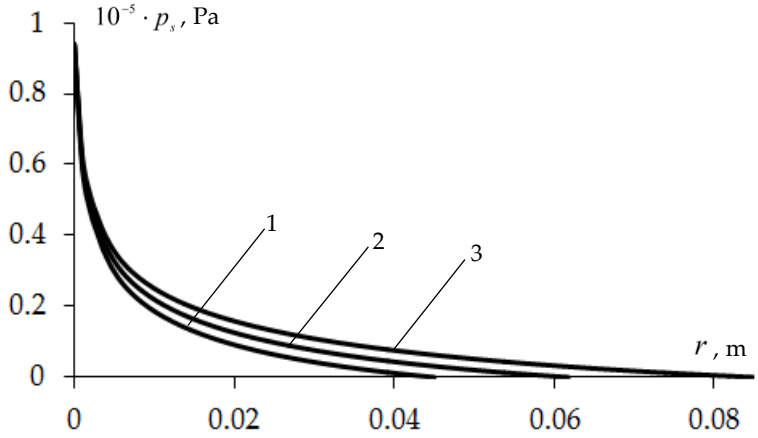


**Figure 2.** The distribution of compression pressure over the thickness of the cake at $t = 450$ (1); 900 (2); and 1800 (3) s., $r = R$ taken as the origin of the distance, $\beta = 0.13$, $\delta = 0.57$, and $p_0 = 10^5$ Pa.

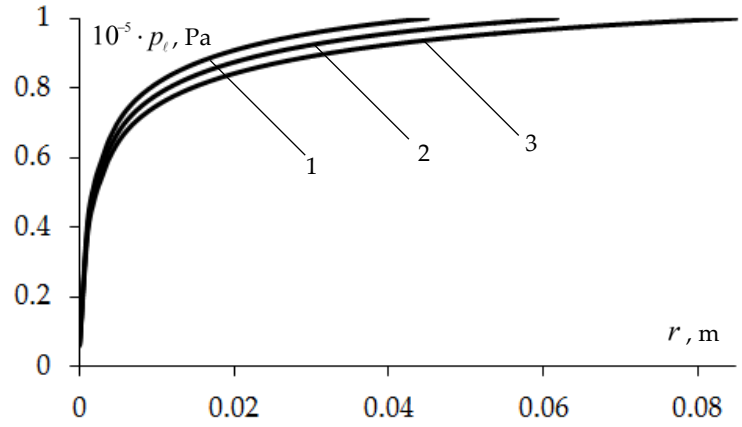


**Figure 3.** The distribution of pressure in the liquid phase $p_\ell$ over the thickness of the cake at $t = 450$ (1); 900 (2); and 1800 (3) s., $r = R$ taken as the origin of the distance, $\beta = 0.13$, $\delta = 0.57$, and $p_0 = 10^5$ Pa.

Figure 4 illustrates the dynamics of the cake thickness $\ell(t) = R_L(t) - R$. One can see its monotonous growth. This is a typical feature of cake filtration [1–3,5,6,11,16,17,20]. In all cases, due to the accumulation of solid particles in the cake on the filter surface despite its compaction (consolidation), i.e., an increase in the concentration of the solid particles and a change in its porosity, the growth of the cake thickness occurs. Of course, the dynamics of this growth are influenced by various factors. Obviously, the compaction of particles in certain areas of the cake slows down the growth of the cake thickness in comparison to a uniform distribution of solid particles. However, this issue should be studied on the basis of a comparison of the solutions to the filtration problems with the formation of the cake, with and without taking into account its consolidation. It is also clear that, with an increase in the liquid supply pressure or an increase in its supply rate, a more progressive development of the cake thickness can be expected. However, in all cases, we obtain monotonically growing dynamics of the cake thickness. The value of $\varepsilon_s$ monotonically decreases from the filter surface to the common boundary of the cake and suspension (Figure 5). As the cake thickness increases over time, one can notice the progress of the distribution profiles $\varepsilon_s$. Due to the densification of the cake, the solids content is higher in the region close to the filter surface. Similarly, it is possible to draw profiles $\varepsilon$, as they have an increasing character in $r$, in accordance with the relation $\varepsilon + \varepsilon_s = 1$.

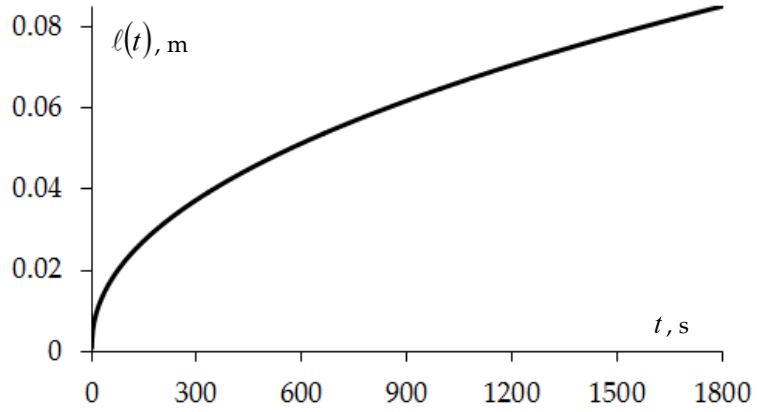


**Figure 4.** Dynamics of the cake thickness on the filter surface, $\beta = 0.13$, $\delta = 0.57$, and $p_0 = 10^5$ Pa.

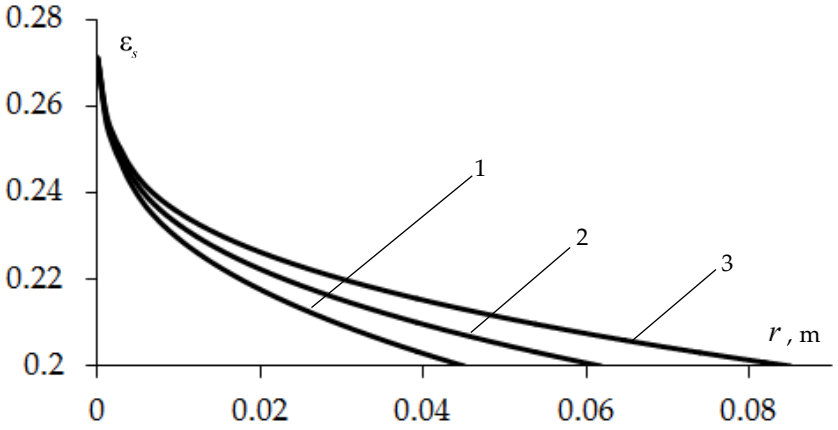


**Figure 5.** Profiles of $\varepsilon_s$ over cake at $t = 450$ (1); 900 (2); and 1800 (3) s., $r = R$ taken as the starting point for distance, $\beta = 0.13$, $\delta = 0.57$, and $p_0 = 10^5$ Pa.

For a given value $\delta$, the distribution of the relative permeability in the cake is shown in Figure 6. As can be seen from the figure, as the cake thickness increases due to the compaction and repacking of the particles and an increase in the compression pressure, the permeability decreases, which can be characterized as an increase in its filtration resistance. This decrease is significant in areas close to the filter surface (small values of $r$ in Figure 6). In this area, a more intensive consolidation of the cake occurs, i.e., the particle compaction is higher. This results in a significant reduction in the relative permeability. At a relatively large $r$, an almost linear decrease in the relative permeability is observed from the common boundary of the suspension and cake towards the filter surface. This may be explained by the slight cake consolidation in these areas. With an increase in the time and a simultaneous increase in the cake thickness, a decrease in the relative permeability is observed over the entire thickness, i.e., consolidation occurs at all points of the cake. In other words, by increasing the time at all the points of the cake, there is an increase in the hydraulic resistance.

The filtration characteristics were calculated for various values of $p_0$. Some results are presented in Figure 7. As can be seen from the graphs, an increase in the supply pressure of the suspension leads to an intensification of the filtering process. The pressure distributions, $p_\ell$ and $p_s$, with higher values are established, with the similarity of the profiles themselves. The increase in the cake thickness also intensifies, and one can notice the leading dynamics of $\ell(t)$ for a large $p_0$.

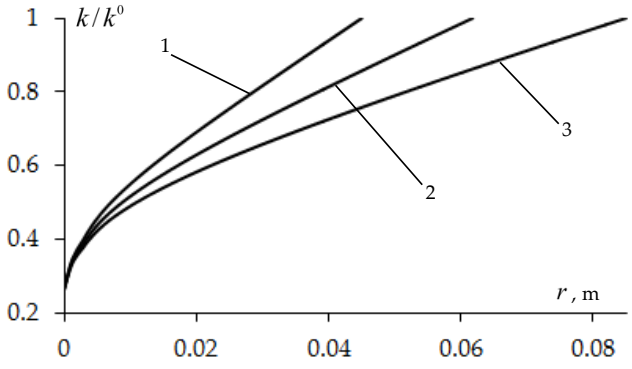


**Figure 6.** Profiles of $k/k^0$ over cake at $t = 450$ (1); 900 (2); and 1800 (3) s., $r = R$ taken as the starting point for distance, $\beta = 0.13$, $\delta = 0.57$, and $p_0 = 10^5$ Pa.

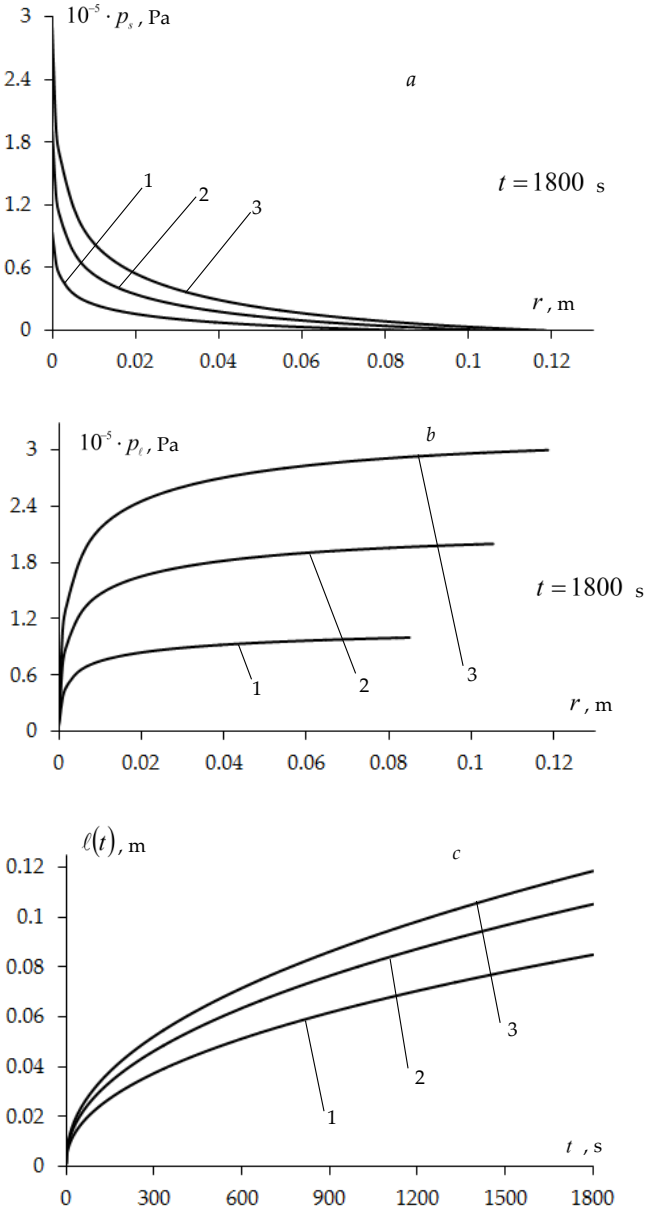


**Figure 7.** Profiles of $p_s$ (**a**), $p_\ell$ (**b**), and the dynamics of the cake thickness (**c**) at $p_0 = 1 \cdot 10^5$ (1); $2 \cdot 10^5$ (2); and $3 \cdot 10^5$ (3) Pa., $\beta = 0.13$, $\delta = 0.57$.

The effect of the parameter δ on the filtering characteristics was also studied (Figure 8). An increase in the value of δ leads to a decrease in the value of $k/k^0$ for the same values of $p_s$ and $k^0$, and this is reflected in the other indicators of filtration. An increase in δ leads to a decrease in the distribution of $p_s$ (Figure 8a). Taking into account the dependence of $p_s + p_\ell = p_0$, $p_0 = \text{const}$, this, in turn, leads to an increase in the values of the distribution $p_\ell$ (Figure 8b). As already mentioned, an increase in the value of δ leads to a decrease in $k/k^0$, which can be interpreted as an increase in the filtration resistance of the cake. With an increase in the filtration resistance, an increase occurs in the $p_\ell$ distribution. Therefore, the increase in $p_\ell$ can be explained by an increase in the filtration resistance of the cake, with an increase in the parameter δ . At the same time, there is a lag in the dynamics of $\ell(t)$, and with relatively large δ, the cake thickness grows slower (Figure 8c). This can also be explained by an increase in the filtration resistance of the cake. The decrease in $k/k^0$ is due to the compaction of the distribution of solid particles in the cake, which reduces its thickness.

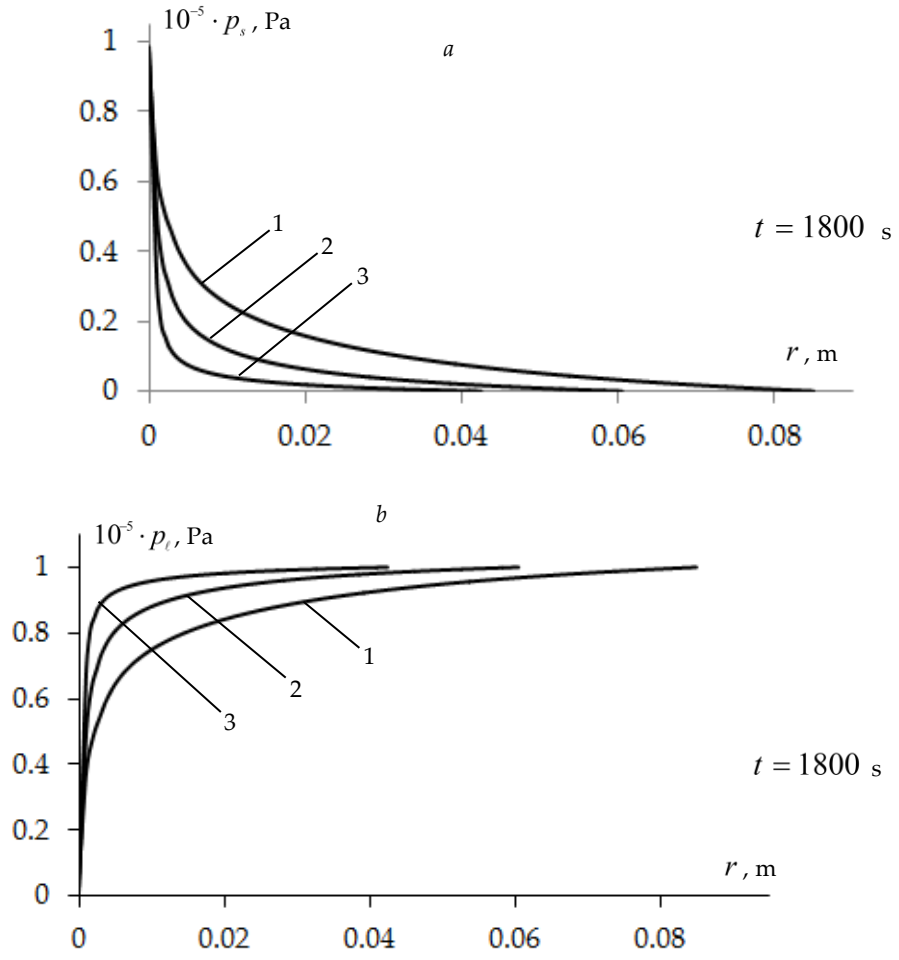


**Figure 8.** *Cont.*

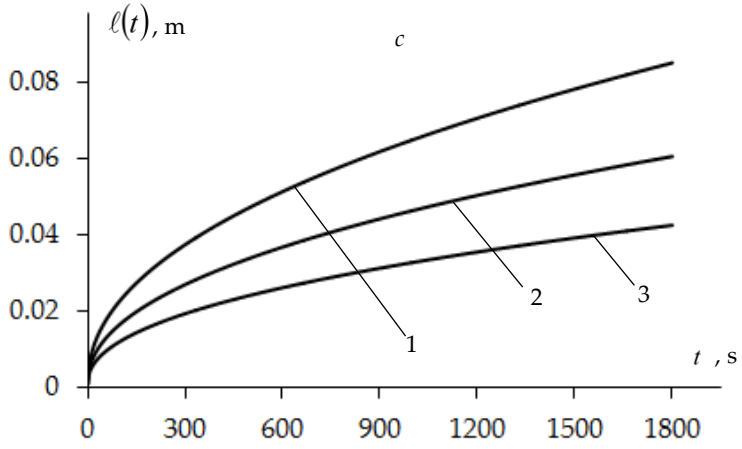


**Figure 8.** Profiles of $p_s$ (**a**), $p_\ell$ (**b**), and the dynamics of the cake thickness (**c**) at $\delta = 0.57$ (1); 1.14 (2); and 2.0 (3), $p_0 = 1 \cdot 10^5$ Pa, $\beta = 0.13$.

Similar calculations have been performed for the various values of parameter β (Figure 9). For large values of this parameter, in accordance with (9), large values of $\varepsilon_s$ can be obtained for the same values of $p_s$ and $\varepsilon_s^0$. Consequently, this results in lower values of $\varepsilon$. A decrease in $\varepsilon$ naturally leads to a decrease in the filtration characteristics of the cake. Thus, a similar effect can be expected with an increase in the parameter δ. The results of the calculation confirm this conclusion. Comparing Figure 7 with Figure 9, we can notice the similar character of the change in $p_s$, $p_\ell$, and $\ell(t)$ with an increase in values of the parameters δ and β.

We compared the behavior of $\ell(t)$ for this radial axisymmetric case and the planar one-dimensional filtering case, with the same parameters used here, except for the geometric parameters (Figure 10). In flat vertical filtering, the cross-section of the cake above the filter does not change. In radial symmetric filtration, the area of the solid particles settling in the form of a cylindrical surface constantly increases with an increasing $\ell(t)$. Therefore, the growth rate of the $\ell(t)$ must decrease. The calculations performed show that the growth occurs in this way. After a certain time, the growth rate of the $\ell(t)$ for the radially symmetric case slows down compared to the flat case.

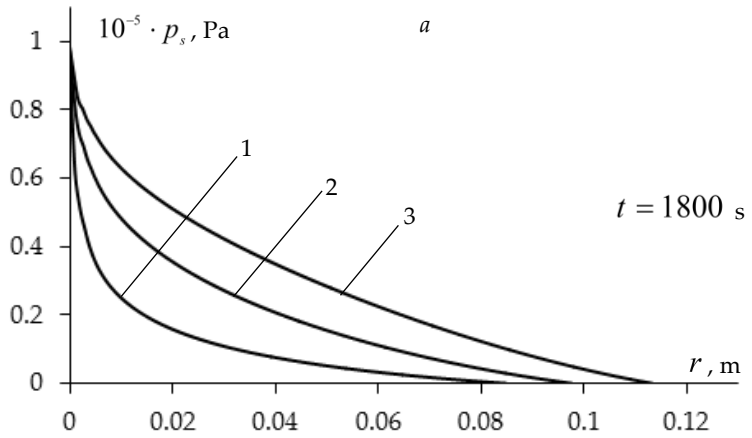


**Figure 9.** *Cont.*

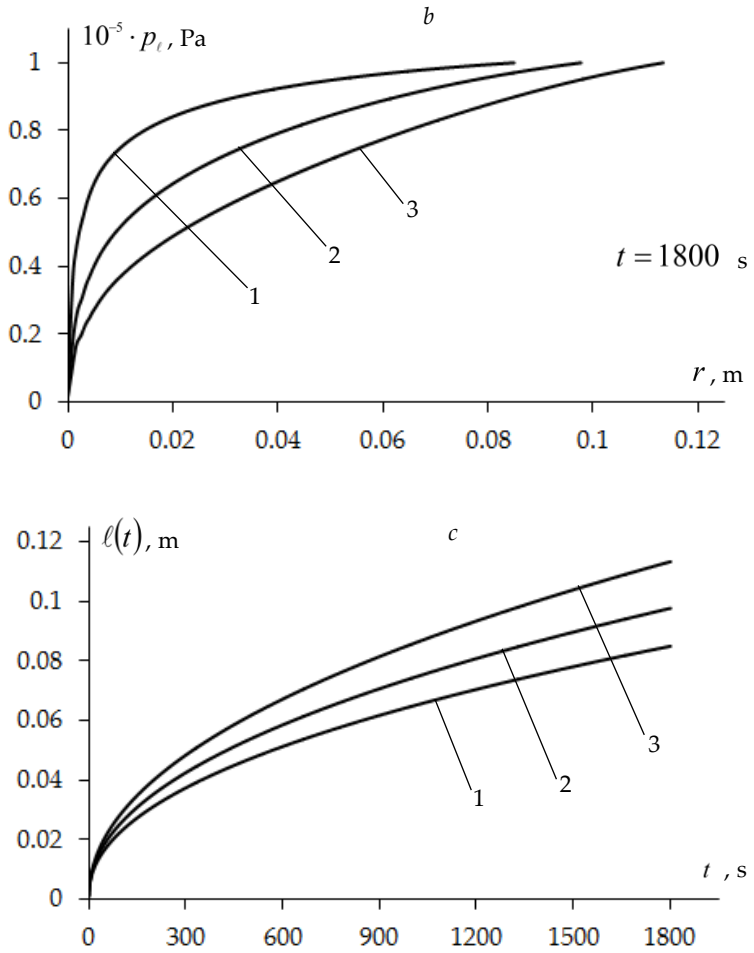


**Figure 9.** Profiles of $p_s$ (**a**), $p_\ell$ (**b**), and the dynamics of the cake thickness (**c**) at $\beta = 0.13$ (1); 0.78 (2); and 1.56 (3), $p_0 = 1 \cdot 10^5$ Pa, $\delta = 0.57$.

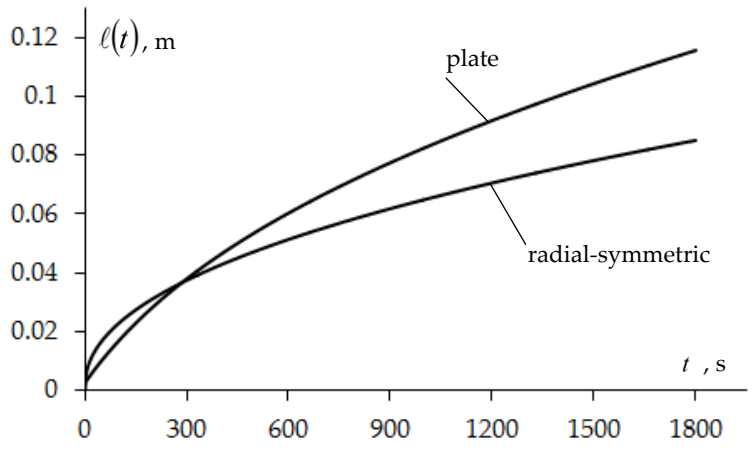


**Figure 10.** Dynamics of the cake thickness for the plate and radial symmetric cases, $p_0 = 1 \cdot 10^5$ Pa, $\beta = 0.13$, and $\delta = 0.57$.

## 6. Conclusions

In this paper, an axisymmetric filtration problem of a suspension with the formation of a cake was considered. It was supposed that a cake was formed on the filter surface, consisting of solid suspension particles. For the equations describing the process, some problems were formulated and some have been solved numerically.

The properties of the cake were characterized by the volume fraction of the particles or the solidosity and cake permeability, which were assumed to be functions of the cake's compressive stress. In particular, power law expressions were used to represent the constitutive relationships for these characteristics. Several values of the parameters in these relationships were used to calculate the filtration characteristics of the cake. The distributions of the compression pressure and the fluid pressure over the cake, as well as the growth of the cake thickness, were determined. The compression pressure decreased from the filter surface to the boundary of the cake and suspension. In contrast, the liquid pressure increased from the value $\Delta p_m$ on the filter surface to the value $p_0$ on the common boundary of the suspension and the cake. The profiles of both the compression pressure and the liquid pressure over the cake had exact ends corresponding to the moving front of the cake. During the filtration process, the thickness of the cake monotonously grew and its solidosity was higher in the region close to the filter surface. Such behavior of the solidosity determined the porosity distribution in the cake. As the solidosity increased from the common boundary of the suspension to the surface of the filter, according to $\varepsilon + \varepsilon_s = 1$, the porosity had a decreasing character from the common boundary of the suspension to the filter surface. Obviously, the decreasing nature of the porosity determined the same nature of the permeability. The increase in the pressure $p_0$ led to the intensification of the pressure distributions $p_\ell$ and $p_s$ and a greater growth of the cake thickness. The influence of the parameters $\delta$ and $\beta$ on the filtration characteristics was also analyzed.

An increase in the value of $\delta$ led to a decrease in the value of $k/k^0$ for the same values of $p_s$ and $k^0$, and this was reflected in the other characteristics of filtration. The decrease in $k/k^0$ could be interpreted as an increase in the filtration resistance of the cake. As a result, the decrease in the distribution of $p_s$ and the increase in the distribution of $p_\ell$ occurred. At the same time, there was a lag in the dynamics of $\ell(t)$, and with a relatively large $\delta$, the cake thickness grew slower. This could also be explained by an increase in the filtration resistance of the cake.

Comparative analyses showed that the behavior of $\ell(t)$ for the radial axisymmetric case and planar one-dimensional filtering case, with the same parameters used except for the geometric parameters, were different. After a certain time, the growth rate of $\ell(t)$ for the radially symmetric case slowed down compared to the flat case.

Thus, one can conclude that the radial axisymmetric filtration model developed in this work can physically and correctly describe the cylindrical filtration involving a cake and the growth of its thickness.

**Author Contributions:** Investigation, B.K.K., G.I., U.S. and B.A.P.; methodology, B.K.K., G.I., U.S. and B.A.P.; project administration, B.K.K. and U.S.; validation, B.K.K., G.I., U.S. and B.A.P.; visualization, G.I.; writing—original draft preparation, B.K.K., G.I., U.S. and B.A.P.; writing—review and editing, B.K.K., G.I., U.S. and B.A.P. All authors have read and agreed to the published version of the manuscript.

**Funding:** The work was partially supported under grant FZ-2020092877, Ministry of innovation development, Republic of Uzbekistan.

**Data Availability Statement:** Not applicable.

**Acknowledgments:** The authors thank anonymous reviewers for their extremely detailed and useful comments.

**Conflicts of Interest:** The authors declare no conflict of interest.

## References

1. Tien, C. *Principles of Filtration*, 1st ed.; Elsevier: Amsterdam, The Netherlands, 2012.
2. Tien, C.; Ramarao, B.V. *Granular Filtration of Aerosols and Hydrosols*; Elsevier Science & Technology Books: Syracuse, NY, USA, 2007; p. 522. [CrossRef]
3. Tien, C. *Introduction to Cake Filtration: Analysis, Experiments, and Applications*, 1st ed.; Elsevier: Amsterdam, The Netherlands, 2006; p. 304.
4. Zhuzhikov, V.A. *Filtration. Theory and Practice of Separation of Suspensions*; Khimiia Publishing: Moscow, Russia, 1980; p. 440.

5. Fedotkin, I.M.; Vorobev, E.I.; Vyun, V.I. *Hydrodynamic Theory of Suspension Filtration*; Vishashkola Publisher: Kiev, Ukraine, 1986; p. 166.
6. Fedotkin, I.M. *Mathematical Modelling of Technological Processes*; Vishashkola Publisher: Kiev, Ukraine, 1988; p. 415.
7. Tien, C.; Bai, R. An assessment of the conventional cake filtration theory. *Chem. Eng. Sci.* **2003**, *58*, 1323. [CrossRef]
8. Iritani, E.; Katagiri, N.; Youshida, T. Simplified Evaluation of Consolidation and Expansion Behaviour of Highly Compressible Cake. *Filtration* **2018**, *18*, 50–60.
9. Burger, R.; Concha, F.; Karlsen, K.H. Phenomenological model of filtration processes. Cake formation and expression. *Chem. Eng. Sci.* **2001**, *56*, 4537–4553. [CrossRef]
10. Vorobiev, E.; Tarasenko, A. Effect of cake compressibility on suspension filtration process regularities. *Theor. Fundam. Chem. Technol. Acad. Sci. USSR* **1987**, *21*, 507–513.
11. Vorobjov, E.I.; Anikeev, J.V.; Samolyotov, V.M. Dynamics of filtration and expression: New methods for combined analysis and calculation of the processes with due to account of the cake consolidation dynamics and the filter medium compressibility. *Chem. Eng. Process.* **1993**, *32*, 45–51. [CrossRef]
12. Vorobiev, E. Nonlinear consolidation model for the prediction of constant pressure expression of semi-solid materials. *Chem. Eng. Sci.* **2021**, *235*, 116458. [CrossRef]
13. Vorobiev, E. Dewatering of non-uniformly structured wet compacts under additional compressive pressure: Predictive model. *Powder Technol.* **2022**, *404*, 117469. [CrossRef]
14. Atsumi, K.; Akiyama, T. A study of cake filtration. Formulation as a Stefan problem. *Chem. Techn.* **1979**, *31*, 487–492.
15. Shirato, M.; Aragaki, T. Verification of internal flow mechahism theory of cake filtration. *Filr. Separ.* **1972**, *3*, 290–297.
16. Smiles, D.E.; Rosental, M.G. The movement of water in swelling materials. *Aust. J. Soil Res.* **1968**, *6*, 237–248. [CrossRef]
17. Wakeman, R.G. A numerical integration of the differential equations describing the formation of and flaw in compressible filter cakes. *Trans. Inst. Chem. Eng.* **1978**, *56*, 258–265.
18. Samarskiy, A.A.; Vabishchevich, P.N. *Computational Heat Transfer*; Editorial URSS: Moscow, Russia, 2003; p. 784.
19. Khuzhayorov, B.K.; Saydullaev, U.; Fayziev, B. Relaxation Equations of Consolidating Cake Filtration. *J. Adv. Res. Fluid Mech. Therm. Sci.* **2020**, *74*, 168–182. [CrossRef]
20. Khuzhayorov, B.K.; Saydullaev, U.; Ibragimov, I.; Wahi, N. An Axisymmetric Problem of Suspension Filtering with Formation of Elastic—Plastic Cake Layer. *Symmetry* **2022**, *14*, 1202. [CrossRef]
21. Kuzmina, L.I.; Osipov, Y.V.; Astakhov, M.D. Filtration of 2-particles suspension in a porous medium. In *Journal of Physics: Conference Series, Volume 1926, Proceedings of the Innovations and Technologies in Construction (BUILDINTECH BIT 2021), Belgorod, Russia, 9 th—10th March 2021*; IOP Publishing: Bristol, UK, 2021. [CrossRef]
22. Duan, C.; Liu, C.; Wang, C.; Yue, X. Numerical methods for porous medium equation by an energetic variational approach. *J. Comput. Phys.* **2019**, *385*, 13–32. [CrossRef]
23. Khuzhayorov, B.K.; Ibragimov, G.; Saydullaev, U.; Shadmanov, I.; Ali, F.M. Filtration of suspensions with forming of an elasto-plastic cake. *Waves Random Complex Media* **2022**, *32*, 1–24. [CrossRef]
24. Bürger, R.; Careaga, J.; Diehl, S.; Pineda, R. Numerical schemes for a moving-boundary convection-diffusion-reaction model of sequencing batch reactors. *arXiv* **2023**, arXiv:2304.07489.